energies

MDPI

Article

An Assessment of the Operation and Emission Characteristics of a Diesel Engine Powered by a New Biofuel Prepared Using In Situ Transesterification of a Dry Spirogyra Algae–Jatropha Powder Mixture

Siddharth Jain

Department of Mechanical Engineering, School of Engineering, University of Petroleum and Energy Studies, Dehradun 248007, India; arthjain2001@gmail.com

Abstract: The present work deals with the optimization of the process parameters of in situ transesterification of dry spirogyra Algae–Jatropha powder along with engine efficiency and combustion analysis of the prepared biofuel. Three operational parameters, namely catalyst concentration (0–5 wt.%), methanol to dry algae–Jatropha curcas powder (*v*/*v*) (20–60%), and reaction time (60–180 min) at a constant reaction temperature of 50 °C, were selected. Response surface methodology (RSM) was used to design the experiments. The maximum biodiesel yield of 88.5% was obtained under the optimized conditions of a catalyst concentration of 3.396% (*w*/*w*), methanol/oil ratio of 19.86, and reaction time of 180 min. At varying loads, the performance and emissions of a diesel engine linked to a power source and fueled with various biodiesel mixes (Diesel, B5, B10, and B20) were tested. It was found that BSFC decreased as the applied load increased for all of the evaluated fuels. All of the biodiesel blends had greater BSFC than the diesel fuel. However, a substantial decrease in the emissions, including hydrocarbon (HC) and carbon monoxide (CO), was observed with the increase in NOx emissions. This method of preparing biodiesel will be beneficial in order to cater to the needs of the transportation sector because it has a lower energy consumption and less engine emissions.

Keywords: biodiesel; engine performance; emissions; algae; jatropha; transesterification

Citation: Jain, S. An Assessment of the Operation and Emission Characteristics of a Diesel Engine Powered by a New Biofuel Prepared Using In Situ Transesterification of a Dry Spirogyra Algae–Jatropha Powder Mixture. *Energies* **2023**, *16*, 1470. https://doi.org/10.3390/en16031470

Academic Editor: Constantine D. Rakopoulos

Received: 16 December 2022
Revised: 19 January 2023
Accepted: 30 January 2023
Published: 2 February 2023

1. Introduction

Industrialization, growing populations, and global economic expansion all contribute to the rapid increase in fossil fuel usage. Alternative energies, including solar, wind, geothermal, and biomass, are available and are being considered [1–4]. Hydrocarbon fuel is the primary source of energy for the world economy. Diesel will certainly account for roughly 60% of the energy increase in 2035, which will be over 80% of the entire energy supply. In future years, it is anticipated that the energy landscape will continue to improve [5–8]. Rapid depletion of fossil fuels and pollution as a result of the Paris Climate Change Agreement have prompted scientists and researchers to develop green alternative fuels capable of meeting the energy demand in a sustainable manner. In the past few decades, oxygenated liquid fuels have shown an acceptable performance, as well as preventing pollution in the environment [9]. There are various oxygenated fuels such as alcohols, biodiesel, and bio-oil that are given more emphasis nowadays due to their promising results [10,11]. Among the alternatives, biodiesel has been shown to be a good substitute for petrochemical diesel in compression ignition engines [12]. The primary advantages of biodiesel are that it is recyclable, reusable, carbon neutral, and it emits no dangerous toxins [13]. Biodiesel is an oxygenated fuel. Triglycerides react with low-molecular alcohols (often methanol) in the presence of a catalyst to produce alkyl ester and glycerol as byproducts, known as transesterification [14].

The chemical constituents of biofuel, which include saturated and unsaturated fatty acids, have a significant impact on the fuel properties [15]. High-saturated fatty acid fuels

have a strong oxidation stability but poor cold flow qualities, whereas high-unsaturated fatty acid fuels with double or triple carbon–carbon bonds have acceptable cold flow capabilities, but poor oxidation stability [16,17]. Oxidation stability refers to the oxidation-resisting tendency of a fuel that occurs during storage. The occurrence of oxidation in biodiesel is caused by the free-radical chain reaction mechanism. The process has three phases in an environment of heat, sunlight, residual metals, and hyper-oxides: activation, spread, and closure. The degree of oxidation varies according to the fatty acid composition. Poor oxidative stability results in gum formation and re-polymerization during storage.

The impact of biofuel on gasoline engine efficiency and emissions has been examined by various researchers by integrating various engine modifications and fuel blends. A substantial reduction in unburnt hydrocarbons (UHC), carbon monoxide (CO), and particulate matter (PM) was reported using biodiesel in IC engines [18,19]. Because of the presence of oxygen inside gasoline, the combustion process generates high temperatures, resulting in a modest rise in nitrogen oxides (NOx) when using biodiesel in comparison with conventional diesel fuel [20–22].

The differences in the physicochemical properties of biofuel derived from different feedstocks have resulted in different trends in engine characteristics [23]. Very few studies have reported the effect of oxidatively stabilized and non-stabilized biodiesel on engine performance and emissions. Poorly stabilized fuel results in the formation of aldehydes, ketones, and more soluble polymers, which consequently increase the density, viscosity, and surface tension of the fuel, thus decreasing the calorific value of the fuel [24]. Non-edible sources that can be obtained from non-agricultural (barren) lands are considered major sources of feedstock for biodiesel production. Jatropha curcas is the most common and promising feedstock to meet the biodiesel demand in India due to because of its abundance [25]. Liu et al. [26] reported that, upon increasing the oxidation duration of jatropha biodiesel, CO_2 and NOx emissions increased rapidly in a diesel engine. Fattah et al. [27] studied the effect of adding antioxidants to a 20% blend of jatropha biodiesel. The results reported that BSFC and BP decreased with the antioxidants when compared with pure 20% jatropha biodiesel. Ryu [28] conducted a study on the influence of five different antioxidants in biodiesel on engine performance and revealed a drop in BSFC for the fuel containing antioxidants compared with the biodiesel without antioxidants.

Jain et al. [29] studied the efficiency and exhaust emissions of oxidatively stabilized jatropha biodiesel. Antioxidants were introduced into the jatropha biodiesel. The study reported an increase in BSFC with and without antioxidants as time passed, but less of an increment was found in the case where antioxidants were present. The reason for this is that stabilized biodiesel has less BSFC compared with non-stabilized biodiesel. CO, HC, and NOx decreased with time. Lower traces of metals in the particulate emissions and a decrease in gaseous emissions, except for NOx, were recorded when using jatropha biodiesel in a four-cylinder DI diesel engine [30]. Rao et al. [31] treated jatropha biodiesel with $Al(OH)_2$ nanoparticles and water and found a significant reduction in gaseous emissions, such as NO, CO, UHC, and others. The addition of nanoparticles increased the storage stability, but the agglomeration of particles occurred, which deteriorated the quality of the fuel [32]. Thus, nanoparticles cannot be used as antioxidants.

From the literature review, it can be found that poor oxidation stability deteriorates the quality of biodiesel. Long-term oxidation results in a poor engine performance and in emissions. Various studies have previously reported that adding antioxidants to biodiesel increased its oxidation stability. However, the use of antioxidants increased the production cost of biodiesel. Jatropha biodiesel consists of 80% unsaturated fatty acids and 20% saturated fatty acids. Sui et al. [33] reported that in jatropha biodiesel, methyl linoleate (42.21%) is the major unsaturated fatty acid responsible for oxidation. To handle this problem, Jatropha curcas oil was blended with algal oil and the blend was then subjected to low temperature transesterification, and this method was proposed as it is a successful method for handling the high unsaturation and high FFA of Jatropha curcas oil in order to make biodiesel [7]. In view of this, in the present work, we proposed reducing the unsaturation

of Jatropha curcas fats with the addition of highly saturated algae fats. Spirogyra algae have been proven to be a potential third-generation feedstock for biodiesel production. The algae consist of 41% saturated and 59% unsaturated fatty acids.

This study examined the in situ transesterification of Jatropha curcas. It is proposed We combined the dried seed powder of Jatropha curcas with dried Spirogyra algae powder to produce a stabilized biodiesel. As the stability of the algae biodiesel was higher than that of the Jatropha biodiesel, the resulting biodiesel had a higher oxidation stability compared with the pure Jatropha curcas biodiesel. The resulting highly stabilized biodiesel was used in the engine to check the performance and emission characteristics.

2. Methods and Materials

2.1. Materials

In this study, algae (spirogyra) were gathered from the Ganga Canal close to the city of Haridwar and Jatropha seeds were bought from the market. Chemicals such as NaOH and methanol were procured from Vikas Scientific Works, Roorkee, India. All of the chemicals were of analytical grade. NaOH (98% pure) was used in pellet form as a base catalyst.

2.2. Fuel Preparation

The spirogyra algae were heated in an oven at 100 °C to remove the moisture content from the algae. The dry algae and jatropha seeds were crushed into powder form. A sample of 5 mg mixture of dry algae–Jatropha powder was used in each experiment (1:1) w/w. The in situ transesterification process was performed with the help of a biodiesel reactor, as shown in Figure 1.

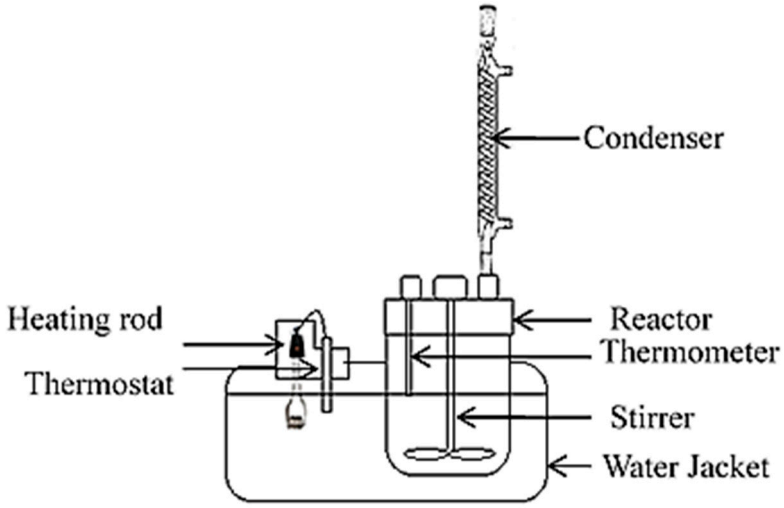

Figure 1. Schematic of the working reactor.

The experiment included the enhancement of three processing parameters, namely the methanol to dry-algae proportion (MDAP) (8, 14, and 20%) (w/w), acid-catalyst (H2SO4), base-catalyst (NaOH), and catalyst concentration (CC) (0, 2.5, and 5%) (w/w) for each, and the reaction time (RT) (60, 120, and 180 min) for the in situ transesterification of dry algae at 50 °C using an RSM-based Box–Behnken configuration. Table 1 depicts the experimental design for optimization studies of several factors in order to achieve a high biodiesel production.

The biodiesel obtained was filtered using qualitative filter paper and distilled water was used to remove the pollutants and glycerin and to obtain pure biodiesel. The schematic of the bioreactor used in this study is shown in Figure 1.

Table 1. Design of experiments for optimization studies considering different parameters.

S. No.	CC (A)	MDAP (B)	RT (C)
1	2.5	20	180
2	2.5	8	180
3	0	14	180
4	5	14	180
5	2.5	14	120
6	0	20	120
7	5	20	120
8	0	8	120
9	2.5	14	120
10	2.5	14	120
11	5	8	120
12	0	14	60
13	2.5	8	60
14	2.5	20	60
15	5	14	60

Statistical Analysis

The examination of the connection between the independent variables and the response yield included three steps: variance analysis (ANOVA), regression analysis, and mapping of the response values. Design Expert 11 was utilized to assess the statistically significant results of the entire quadratic polynomial model with a 95% confidence level ($p = 0.05$). The response values of the trials were determined by the highest values for the empirical yield%. Then, the developed model was employed for analyzing the interactive effect of each variable. Surface regression analysis was performed using the polynomial equation (Equation (1)):

$$Y = \beta_0 + \sum_{j=1}^{k} \beta_j X_j + \sum_{j=1}^{k} \beta_{jj} X_j^2 + \sum_{i=1}^{j-1} \sum_{i=2}^{k} \beta_{ij} X_i X_j + \varepsilon \quad (1)$$

In which Y is the result (% Fatty-acid methyl ester production); i and j are the quadratic and linear coefficient, respectively; X_i and X_j are the un-coded independent variables; ε is the random disturbance term; k is the number of independent factors maximized in the test, ($k = 3$ in this study); and β_0 is the regression coefficient.

2.3. Fuel Characteristics of Biofuel Synthesized

The biofuel characteristics that were derived were measured according to the recognized standards as per Table 2.

Table 2. Fuel characteristics of the prepared biofuel.

Fuel Properties	Standards
Density (kg/m^3)	ASTM D1298
Viscosity (cst) @ 40 °C	IS1448
Flash Point (°C)	IS1448
Calorific value (MJ/kg)	ASTM D4809
Induction period	EN14112

2.4. Experimental Setup

Table 3 lists the technical details of the test engine. The engine was coupled to a KBM-102 2 kVA single-phase synchronous machine. A resistive load panel with a voltmeter, ammeter, wattmeter, and energy meter was manufactured. This panel's load capacity was maintained at 2 kW. The unit for measuring fuel was a graded clear glass cylinder. The bottom end of the cylinder was equipped with a stopcock, but the top end was open. A PVC pipe was used to link the stopcock's output to the diesel engine's filter unit. The HC, CO, NOx, and O_2 tailpipe emissions were measured using a technique developed by FMTechnologies. The experimental engine configuration is seen in Figure 2 and the engine's geometric characteristics are listed in Table 3.

Table 3. Specific technical characteristics of the testing apparatus.

Engine Variables	Specifications
Supplier	Kirloskar Oil Engines Ltd., Pune, India
Engine type	AA35 single-cylinder, vertical, 4 stroke, single acting high-speed CI-diesel engine
Bore	30.00 mm
Stroke	76.00 mm
CC	0.3820 L
CR	15.60:1
Constant Speed	1500 rpm

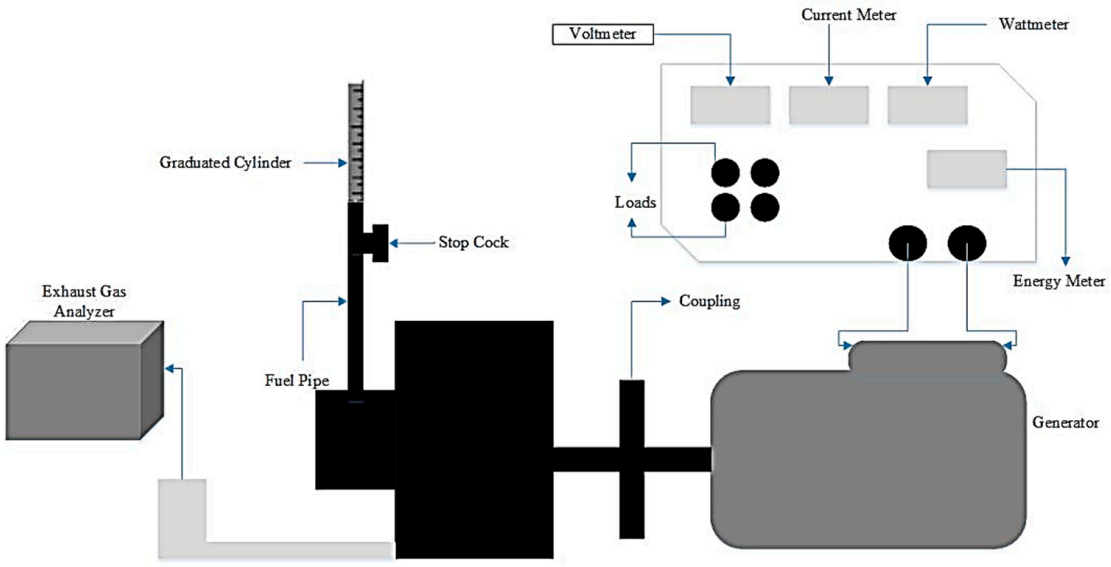

Figure 2. Schematic of the testing setup.

2.5. Experimental-Test Procedure

In the present investigation, B5, B10, and B20 blended fuels were examined under various engine loads ranging from 0% to 100% load with a 25% load interval. All of the mixtures were evaluated under identical conditions, ranging from no load to full load, at a constant speed of 1500 rpm. The diesel fuel was purchased from a gas station in Roorkee. The biodiesel's effects on the engine characteristics were compared to those of pure diesel. Table 4 summarizes the typical fuel parameters of the diesel and biodiesel mixtures. Throughout the warm-up phase, diesel fuel was used at a steady speed and 50% load. In addition, adequate time was allowed for the engine to utilize the existing diesel in the fuel delivery system before testing additional fuel.

Table 4. Fuel properties of the fuel used.

Fuel Properties	Diesel	B5	B10	B20
Density (kg/m^3) @ 40 °C	0.834	0.836	0.839	0.844
Viscosity (cst) @ 40 °C	3.21	3.25	3.29	3.37
Flash Point (°C)	76	78	80	85
CV (MJ/kg)	44.50	44.375	44.25	44.0

3. Results and Discussion

3.1. Transesterification Process

In the procedure of transesterification, two distinct response yields were achieved, namely the experimental value and the projected value. The experimental yield was determined by executing 15 separate tests, whereas the projected yield was determined by employing RSM. These two response yields are expressed as a percentage, and the three independent process variables (A) catalyst concentration (CC), (B) methanol to dry algae ratio (MDAR), and (C) reaction time (RT) are listed in Table 5. Using multiple regression analysis on the experimental response, the connection between the experimental response and the input parameters was described using second-order polynomial equations containing interaction terms. The complete models developed in coded factors are represented by Equation (2).

$$\text{Yield } \% = 156.51023 + 20.38367 \times A - 2.96322 \times B - 2.13976 \times C - 0.477667 \times A \times B + 0.117767 \times A \times C + 0.031549 \times B \times C - 5.61447 \times A^2 + 0.060197 \times B^2 + 0.006030 \times C^2 \quad (2)$$

where A is RT, B is MDAR, and C is CC.

Table 5. Responses for transesterification of the blend (waste cooking oil + algae oil).

S. No.	CC (A)	MDAR (B)	RT (C)	Yield
1	2.5	20	180	87.56
2	2.5	8	180	40.2
3	0	14	180	22.51
4	5	14	180	58.6
5	2.5	14	120	45.2
6	0	20	120	23.65
7	5	20	120	6.12
8	0	8	120	2.43
9	2.5	14	120	46.29
10	2.5	14	120	41.63
11	5	8	120	13.56
12	0	14	60	38.69
13	2.5	8	60	71.63
14	2.5	20	60	73.56
15	5	14	60	4.12

A graph was plotted between the predicted value and the actual value of the response yield (%), as shown in Figure 3. The graph shows that the predicted values around the zero-error line were scattered at lower values of yield, with some of the points with higher yield values being near to the experimental values. Therefore, this confirms the reliability of the model developed in order to set up a correlation between the response yield of the oil blend and the three independent process variables.

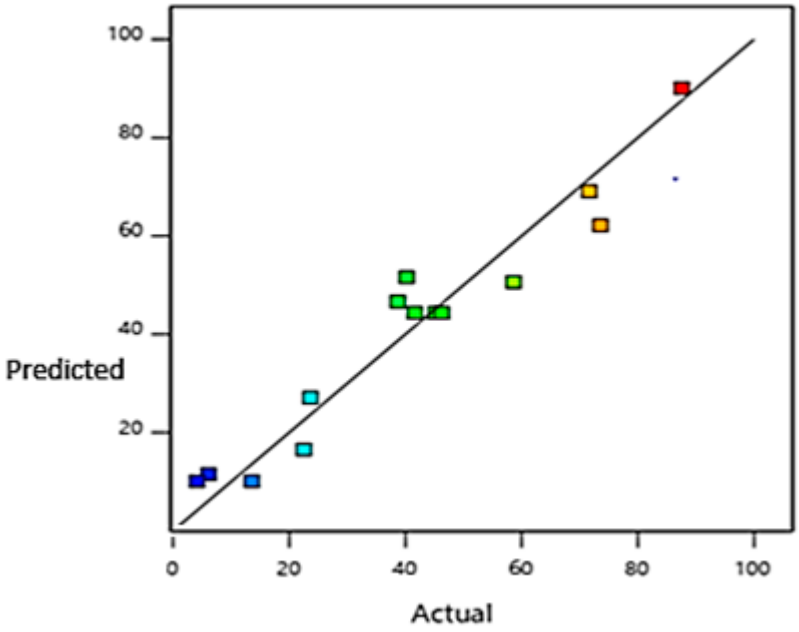

Figure 3. Percentage values of anticipated vs. actual yields.

3.2. ANOVA

The analysis of variance (ANOVA) provides the most reliable approach for measuring the precision of prepared trials and models. Table 6 shows the analysis of variance of the experimental study performed here. The quadratic model that was formed was analyzed using RSM. The model was found to be significant and the lack of fit was insignificant. The appropriateness of the model was evaluated further by calculating the correlation coefficient (R^2). Specifically, a model was appropriate if the regression coefficient was greater than 0.95, indicating that the model could explain up to 95% of the data variability. A R^2 score of 0.99 indicated that the anticipated and experimental results were in excellent agreement. In addition, the projected R^2 and corrected R^2 values agreed rather well.

Table 6. Assessment of the RSM model.

S.No.	Variable	Values
1.	Model	Significant
2.	Lack of fit	Non-Significant
3.	R^2	0.99
4.	Adjusted R^2	0.97
5.	Predicted R^2	0.90

3.3. Influence of Processing Parameters on Output

Referring to Figure 4, this is a perturbation plot of the biodiesel yield concerning the process variables, i.e., catalyst concentration (B), methanol/dry powder ratio (C), and reaction time on the yield percentage of the biodiesel. It was found that the yields first rose quickly with an increase in the amount of catalyst and then began to decrease beyond the increased yield point. It could be that the increased amount of catalyst accelerated the reaction of triglycerides, thereby increasing the biofuel production. Because of an increase in the exchange rate of fatty acids as the reaction time increased, the yields rose and then fell after a certain value. As the transesterification reaction could be reversed, more alcohol needed to be injected to guarantee that all of the triglycerides were converted. Thus, the production of biofuel grew as the amount of methanol increased.

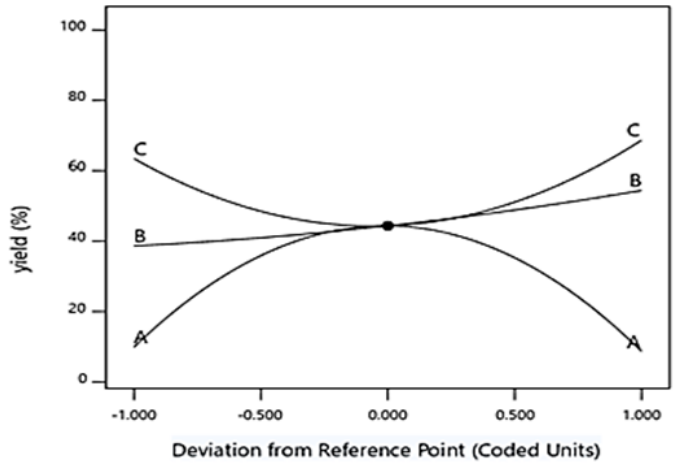

Figure 4. Effect of CC, RT, and MDAR (%).

3.4. Effect of Reaction Parameters on Yield%

Using a modest ellipse inside the contour graphic, software design expert 11 assisted in obtaining the expected output. Using two variables simultaneously, the maximum-yield 3D response curves were produced. The variables in the process were A, B, and C.

The figure shows a response surface representation of the yield versus methanol/dry powder ratio and catalyst. It is represented as process variables "A and B". It was discovered that the yield of the biofuel was affected by two process variables: the methanol/dry powder ratio and the catalyst. The conclusion suggests that the yield of the biofuel grew when the "A and B" process variables increased, i.e., the methanol/dry powder ratio and catalyst. Figure 4 shows a surface representation of the yield versus catalyst and reaction time. It is represented as process variables "A and C". It is shown that the yield of the biodiesel depended on two process variables, i.e., catalyst and reaction time. It was concluded that the yield of the biodiesel increased with the increase in the "A and C" process variables, i.e., catalyst and reaction time. In Figure 5, a response surface representation of the yield versus methanol/dry powder ratio and time is shown. It is represented as process variables "B and C". It is shown that the yield of the biodiesel depended on two process variables, i.e., the methanol/dry powder ratio and time. We concluded that the yield of the biodiesel increased with the increase in "A and C" process variables, i.e., methanol/dry powder ratio and time. Thus, it can be concluded from Figures 5–7 that the surface-confined area within the shortest ellipses in the contour graphs represents the highest projected yield. There is a relationship between these two independent factors that has an impact on the dependent variable (biodiesel yield).

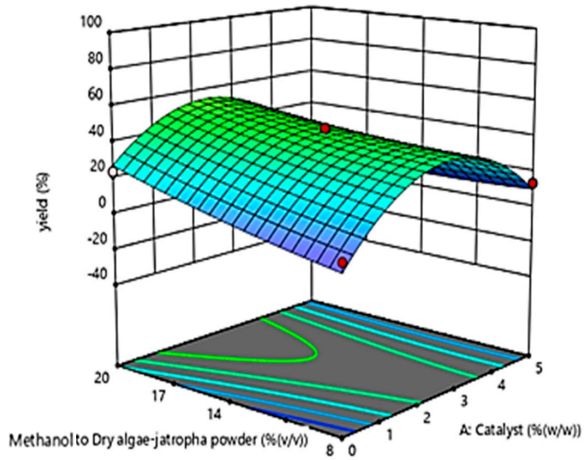

Figure 5. Biodiesel yield (%) vs. catalyst amount (%) and methanol/oil ratio (%).

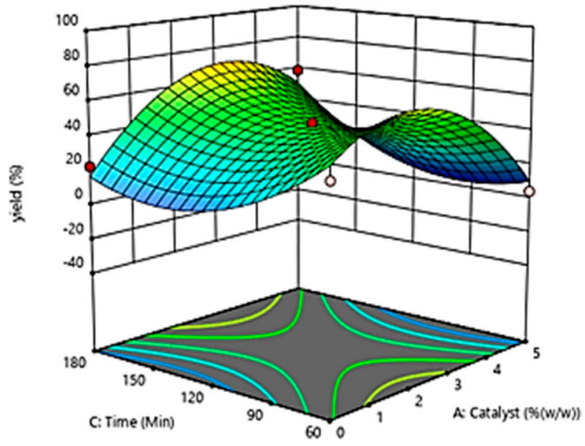

Figure 6. Biodiesel yield (%) vs. catalyst concentration (%) and reaction time (min).

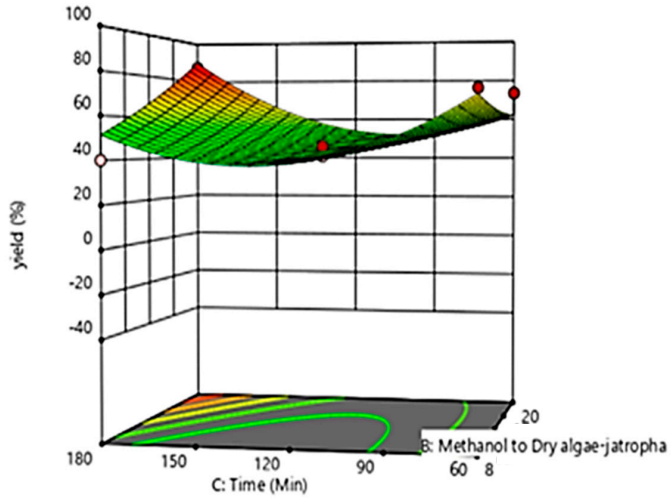

Figure 7. Biodiesel yield (%) vs. methanol/oil ratio (%) vs. reaction time (min).

4. Improvement in Yield Response

In addition, for each answer, an optimization procedure was carried out to maximize the response yield of the mix. The optimization approach was based on the RSM-50 °C.veloped quadratic model (Equation (2)). Table 7 displays the optimal input processing parameters for optimizing biodiesel production, which is 88.5% based on the optimal input process parameter values. To confirm the outcomes, the research was carried out using the improved process parameter values presented in Table 7. In addition, it was found that the projected optimum response was more in line with the empirical optimal response, with an error of 3.5%, as shown in Table 8. In conclusion, the response yield of the biofuel was 92% employing a methanol concentration of 19.86% and 3.396% *w*/*w* NaOH catalyst for 180 min at 50 °C. The physicochemical parameters of the biofuel samples were evaluated in accordance with ASTM D-6751 and IS-15607. These attributes are shown in Table 9.

Table 7. Optimizing parameters for the optimal biofuel production.

Parameters	Objectives	Optimized-Value RSM
Reaction time	In range	180
Methanol concentration	Minimize	19.86%
Catalyst amount	In range	3.396%
Biodiesel yield	Maximize	88.5%

Table 8. The model evaluation at the optimized conditions.

Number	Methanol Concentration (%)	Reaction Temperature (°C)	Catalyst Loading (wt.%)	Reaction Time (min)	Predicted Biodiesel Yield (%)	Experimental Biodiesel Yield (%)	Error (%)
1	19.86	50	3.396	180	88.5	92	3.5

Table 9. Fuel attributes of the produced biofuel.

Fuel Charecterstics	B100	Standards
Density (kg/m^3)	0.8840	ASTM D1298
Viscosity (cst) @ 40 °C	4.00	IS-1448
Flash Point (°C)	116.0	IS-1448
Calorific value (MJ/kg)	42.00	ASTM-D4809
Induction-period	3.20	EN-14112

4.1. Fuel Properties of Biodiesel

The kinematic viscosity of oil is a factor that plays a major role when using the engine. The high value of kinematic viscosity may lead to poor atomization, which may lead to incomplete combustion, which tends to decrease engine performance and increase emissions. The viscosity of biodiesel was found to be 4.0 cSt, which was higher than for diesel. The flashpoint of biodiesel was recorded to be 116 °C, which was far more superior than diesel. The energy content of fuel significantly influences the fuel consumption and the thermal efficiency of the engine. The calorific value of biodiesel was measured as 42.0 MJ/kg. The properties depict that the fuel was compatible with the diesel engine. The properties of the fuels produced were measured according to standard and are shown in Table 9. The table shows the properties of the fuel used in the IC Engine.

4.2. Engine Performance Characteristics

4.2.1. Brake Specific Fuel Consumption (BSFC)

The impact of improved biodiesel fuel characteristics on engine performance and emissions was assessed and compared to diesel. BSFC was calculated and analyzed as shown in Figure 8. It was observed that BSFC for all of the tested fuels decreased with a corresponding increase in load. At lower engine loads or when idle, the majority of the energy produced was needed in order to overcome the frictional resistance of the engine elements. Consequently, BSFC was greater at lower engine loads and decreased as the engine loads grew.

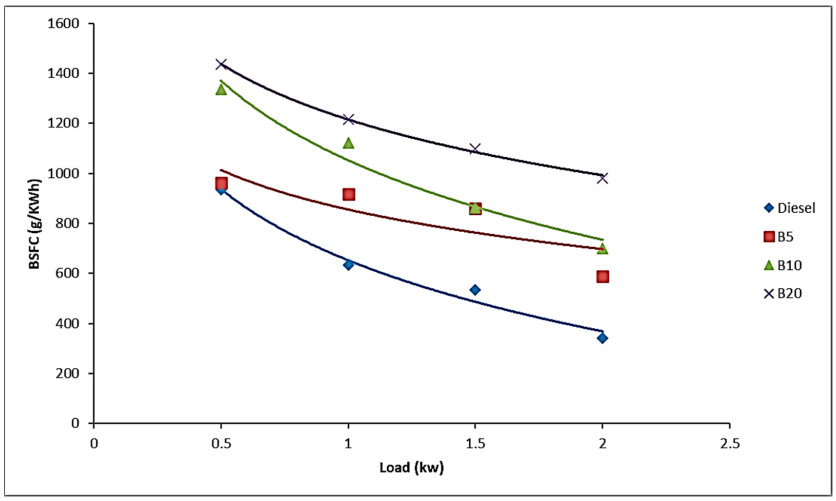

Figure 8. Variation in BSFC with respect to load.

The BSFC values of all of the biodiesel fuels exhibited an upward trend when the biodiesel-to-diesel blending ratio increased. The reason behind this could be attributed to the lower energy content of biodiesel blends per unit mass compared with diesel, meaning more biodiesel fuel was consumed to produce a similar output as in the case of diesel [34]. The results show that B20 showed the best BSFC in comparison with other blended biofuels, which observed a reduction in the calorific value of the fuel with an increase in the blend proportion [35]. The other reason could be the higher density of the biodiesel. At a uniform inlet pressure and constant time, the amount of blended fuel in the injector increased compared with diesel.

4.2.2. Brake Thermal Efficiency

The ratio of brake power output to energy consumed to generate power is known as brake thermal efficiency (BTE) [36]. As shown in Figure 9, BTE increased with increasing the load (%) for all of the fuels tested. The BTE increased for all of the fuels with an increase in load conditions. The increase in BTE at higher engine loads was caused by a reduction in power loss due to friction and an increase in brake power as the engine load percentage increased [37]. Although BTE increased for biodiesel blends with the load, it was lower than diesel at all of the loads. The biodiesel contained inherent oxygen, due to which proper combustion took place, but the decreasing effect of BTE might be attributed to the combined effect of the low calorific value of biodiesel and the higher BSFC than diesel [38].

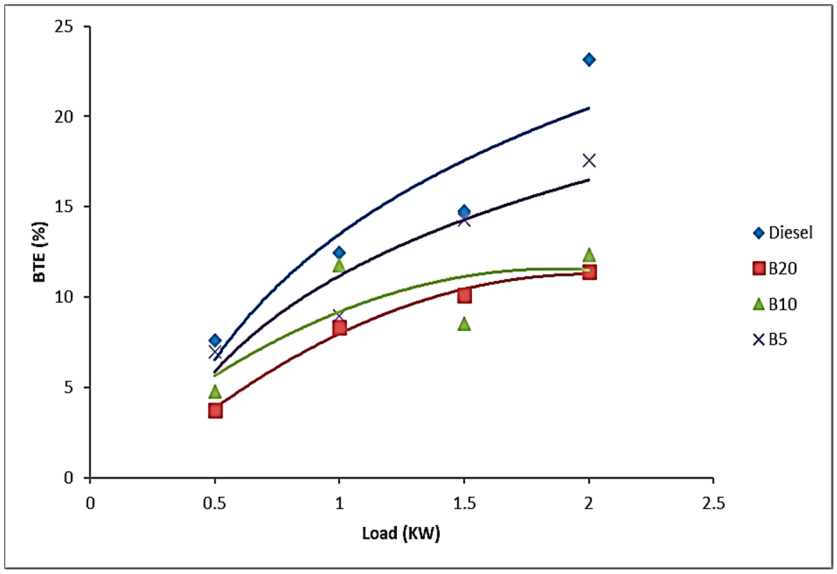

Figure 9. BTE vs. load graph.

In Figure 9, the results indicate that the use of B5 provided the optimum BTE for all of the tests, whereas B20 provided the lowest BTE when compared with other biofuels. This could be due to an increase in the kinematic viscosity of the fuel with an increase in the blend percentage, which tended to lead to poorer atomization, resulting in a poor combustion process and reduced thermal efficiency.

4.3. Properties of Emanation

4.3.1. Hydrocarbon Emissions (HC)

All of the biodiesel blends were found to have extremely low hydrocarbon emissions compared with diesel fuel. Figure 10 displays the variance in HC emissions across all loads and fuels that were evaluated. It can be observed that HC emissions decreased as the load conditions increased. In the case of biodiesel blends, the highest HC emissions were recorded by B5, whereas B20 recorded the lowest amount of HC emissions. This implies that the use of biodiesel significantly reduces HC emissions. This decrease is as

a result of the presence of abundant oxygen, which maintains sufficient oxidation [39]. The temperature increase prevalent in the combustion process as a result of enhanced combustion promotes enhanced fuel evaporation and a reduction in HC emissions. It can be observed from the results that HC emissions decreased more in the case of higher blends.

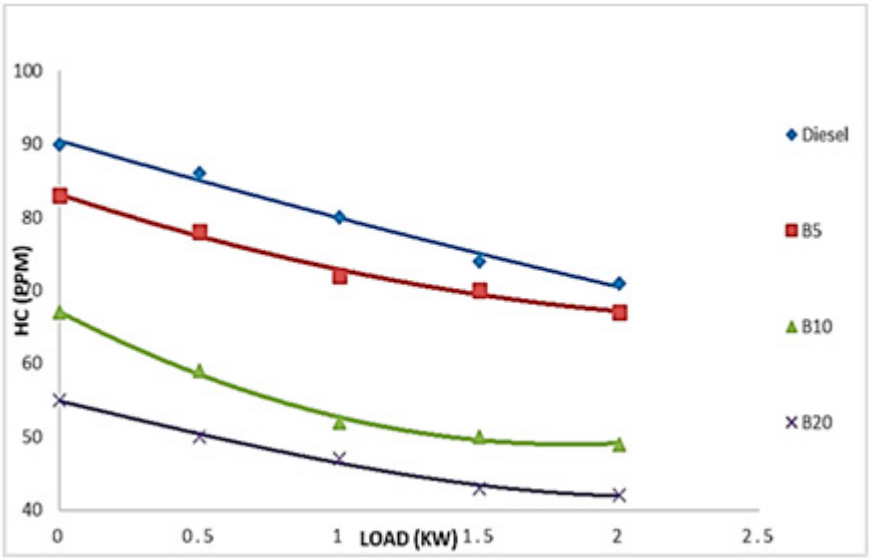

Figure 10. Variation in HC with respect to load.

4.3.2. O_2 Emissions

The composition of inherent oxygen in biodiesel fuel is the most influential property. The presence of excess oxygen improves the combust efficiency of the fuel, which reduces pollutants as a consequence when compared with diesel fuel. Figure 11 represents the O_2 emissions concerning increasing the load for all of the fuels tested. The observation revealed that the O_2 emissions significantly decreased upon use, as well as increased in load circumstances, and the biodiesel blends outperformed the diesel. At lower loads, B5 reported slightly higher O_2 emissions than the other biodiesel blends. At full load conditions, B20 and B5 reported minimum O_2 emissions.

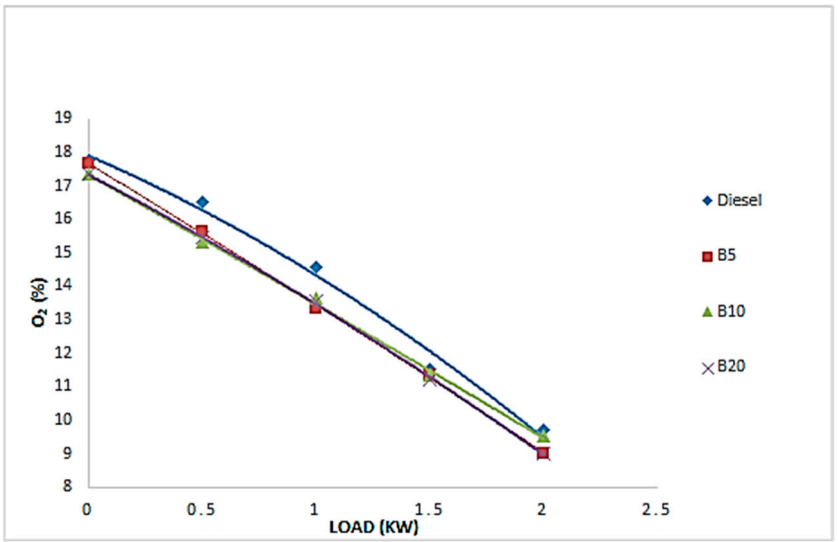

Figure 11. Variation in O_2 with respect to load.

4.3.3. CO Emissions

CO emission originate from partial oxidizing during inadequate combustion [40]. Figure 12 depicts the carbon monoxide emissions of diesel and biodiesel mixtures. It can be seen that at lower loads, CO emissions were high, but with the increase in load condition, the CO emissions tended to decrease. All of the biodiesel blends reported lower CO emissions than for diesel fuel at all of the load conditions. The lowest amount of emissions was recorded at full load conditions. CO emissions were reduced when the biodiesel blend percentage increased. As explained earlier, this could contribute to the high oxygen content of the blends and proper burning when using biofuel.

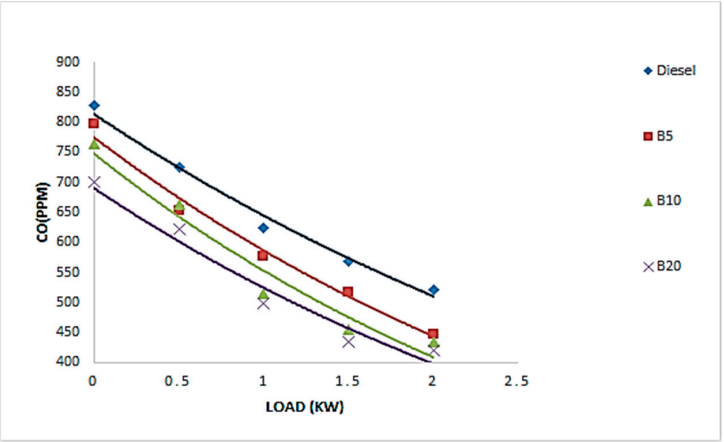

Figure 12. Variation in CO with respect to load.

4.3.4. Nitrogen Oxides (NOx) Emissions

NOx emissions are highly sensitive to a rise in combustion temperature with the increase in oxygen concentration in fuel and engine load [41]. In a high-temperature chamber, the nitrogen molecular bonds break down and form sequential oxidation reactions to form NOx [42]. Figure 13 represents the results of NOx emissions for all of the fuels and shows that the NOx emissions increased with an increase in engine load for all of the tested fuels. For higher biodiesel blends, the oxygen content of the fuel also increased. The results reported in this study also show that the NOx emissions for biodiesel blends were higher than the diesel at all of the load conditions. B20 exhibited more NOx emissions than some other blended fuels because of an increase in oxygen concentration as the biofuel concentration increased.

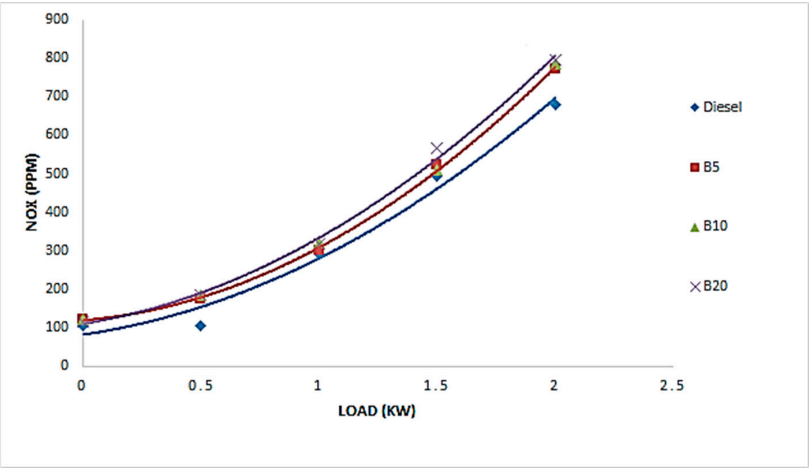

Figure 13. NOx vs. load variation.

5. Conclusions

This study focused on the single-step in situ transesterification of dry spirogyra algae and Jatropha powder, and the engine efficacy and emission analysis of that biofuel prepared using a homogeneous base catalyst. Three operational parameters, including catalyst concentration (0–5 wt.%), methanol to dry algae–Jatropha curcas powder (*v*/*v*) (20–60%), and reaction time (60–180 min) at a constant reaction temperature of 50 °C were selected. The maximum biodiesel yield of 88.5% was obtained under the optimized conditions of a catalyst concentration of 3.396% (*w*/*w*), methanol/oil ratio of 19.86, and reaction time of 180 min. From the engine tests, the following conclusions were drawn:

- It was noted that the BSFC for all of the test blends decreased as the load increased. All of the biodiesel blends reported a higher BSFC compared with diesel fuel. The reason behind this may be that, because of the lower energy content of biodiesel blends per unit mass compared with diesel, more biodiesel fuel is consumed to generate the same power as in the case of diesel.
- B5 reported the highest BTE among all of the tested blends, whereas B20 reported the lowest BTE compared with other fuels. This can be accounted for due to an increase in the kinematic viscosity of the fuel with an increase in the blend percentage, which tends to result in poorer atomization and a proper air−fuel mixture, resulting in a poorer combustion process and reduced thermal efficiency.
- It can be shown that HC emissions decrease as the load conditions increase. In the case of biodiesel blends, the highest HC emissions were recorded by B5, whereas B20 recorded the lowest amount of HC emissions. This implies that the use of biodiesel significantly reduces HC emissions. This occurs due to the presence of excess oxygen, which maintains adequate oxidation.
- All of the biodiesel blends reported lower CO emissions than for diesel fuel at all of the engine loads. At full load, the least amount of emissions was recorded. CO emissions decreased with the increase in the biodiesel blend percentage. As explained earlier, this can be attributed to the higher oxygen content of the blends and proper combustion when compared with diesel.
- According to the findings of this investigation, the NOx emissions of biodiesel blends were greater than those of diesel under all load circumstances. B20 emitted more NOx emissions than other blends due to an increase in oxygen concentration as the biodiesel percentage increased.

From the above, it is found that this new approach of making biodiesel will be useful as Jatropha biodiesel can be used to produce biodiesel with algae. On the other hand, the engine performance and emissions are also comparable with diesel.

Funding: This research received no external funding.

Acknowledgments: The author is grateful to my parent institute for providing research facilities.

Conflicts of Interest: The author declare no conflict of interest.

References

1. Saini, M.; Sharma, A.; Singh, V.P.; Dwivedi, G.; Jain, S. Advancement in Materials, Manufacturing and Energy Engineering. *Adv. Mater. Manuf. Energy Eng.* **2022**, *2*, 310–325. [CrossRef]
2. Jain, S.; Sharma, M.P. Oxidation, Thermal, and Storage Stability Studies of Jatropha Curcas Biodiesel. *ISRN Renew. Energy* **2012**, *2012*, 861293. [CrossRef]
3. Singh, V.P.; Jain, S.; Gupta, J. Analysis of the effect of variation in open area ratio in perforated multi-V rib roughened single pass solar air heater—Part A. *Energy Sources Part A Recover. Util. Environ. Eff.* **2022**, 1–21. [CrossRef]
4. Singh, V.P.; Jain, S.; Gupta, J. Analysis of the effect of perforation in multi-v rib artificial roughened single pass solar air heater—Part A. *Exp. Heat Transf.* **2021**, *36*, 163–182. [CrossRef]
5. World Energy Council. *World Energy Issues Monitor 2020*; World Energy Council: London, UK, 2020.
6. Singh, V.P.; Jain, S.; Karn, A.; Dwivedi, G.; Kumar, A.; Mishra, S.; Sharma, N.K.; Bajaj, M.; Zawbaa, H.M.; Kamel, S. Heat transfer and friction factor correlations development for double pass solar air heater artificially roughened with perforated multi-V ribs. *Case Stud. Therm. Eng.* **2022**, *39*, 102461. [CrossRef]

7. Kumar, S.; Jain, S.; Kumar, H. Application of adaptive neuro-fuzzy inference system and response surface methodology in biodiesel synthesis from jatropha–algae oil and its performance and emission analysis on diesel engine coupled with generator. *Energy* **2021**, *226*, 120428. [CrossRef]
8. Singh, V.P.; Jain, S.; Kumar, A. Establishment of correlations for the thermo-hydraulic parameters due to perforation in a multi-V rib roughened single pass solar air heater. *Exp. Heat Transf.* **2022**, 1–20. [CrossRef]
9. Knothe, G.; Razon, L.F. Biodiesel fuels. *Prog. Energy Combust. Sci.* **2017**, *58*, 36–59. [CrossRef]
10. Dabros, T.M.; Stummann, M.Z.; Høj, M.; Jensen, P.A.; Grunwaldt, J.-D.; Gabrielsen, J.; Mortensen, P.M.; Jensen, A.D. Transportation fuels from biomass fast pyrolysis, catalytic hydrodeoxygenation, and catalytic fast hydropyrolysis. *Prog. Energy Combust. Sci.* **2018**, *68*, 268–309. [CrossRef]
11. McCormick, R.L.; Ratcliff, M.A.; Christensen, E.; Fouts, L.; Luecke, J.; Chupka, G.M.; Yanowitz, J.; Tian, M.; Boot, M. Properties of Oxygenates Found in Upgraded Biomass Pyrolysis Oil as Components of Spark and Compression Ignition Engine Fuels. *Energy Fuels* **2015**, *29*, 2453–2461. [CrossRef]
12. Yesilyurt, M.K.; Cesur, C.; Aslan, V.; Yilbasi, Z. The production of biodiesel from safflower (*Carthamus tinctorius* L.) oil as a potential feedstock and its usage in compression ignition engine: A comprehensive review. *Renew. Sustain. Energy Rev.* **2019**, *119*, 109574. [CrossRef]
13. Jacob, A.; Ashok, B.; Alagumalai, A.; Chyuan, O.H.; Le, P.T.K. Critical review on third generation micro algae biodiesel production and its feasibility as future bioenergy for IC engine applications. *Energy Convers. Manag.* **2020**, *228*, 113655. [CrossRef]
14. Singh, D.; Sharma, D.; Soni, S.; Sharma, S.; Sharma, P.K.; Jhalani, A. A review on feedstocks, production processes, and yield for different generations of biodiesel. *Fuel* **2019**, *262*, 116553. [CrossRef]
15. Jain, S.; Sharma, M. Stability of biodiesel and its blends: A review. *Renew. Sustain. Energy Rev.* **2010**, *14*, 667–678. [CrossRef]
16. Jain, S.; Sharma, M. Effect of metal contents on oxidation stability of biodiesel/diesel blends. *Fuel* **2014**, *116*, 14–18. [CrossRef]
17. Christensen, E.; McCormick, R.L. Long-term storage stability of biodiesel and biodiesel blends. *Fuel Process. Technol.* **2014**, *128*, 339–348. [CrossRef]
18. Deshmukh, S.; Kumar, R.; Bala, K. Microalgae biodiesel: A review on oil extraction, fatty acid composition, properties and effect on engine performance and emissions. *Fuel Process. Technol.* **2019**, *191*, 232–247. [CrossRef]
19. Mahmudul, H.; Hagos, F.; Mamat, R.; Adam, A.A.; Ishak, W.; Alenezi, R. Production, characterization and performance of biodiesel as an alternative fuel in diesel engines—A review. *Renew. Sustain. Energy Rev.* **2017**, *72*, 497–509. [CrossRef]
20. Wei, L.; Cheng, R.; Mao, H.; Geng, P.; Zhang, Y.; You, K. Combustion process and NOx emissions of a marine auxiliary diesel engine fuelled with waste cooking oil biodiesel blends. *Energy* **2018**, *144*, 73–80. [CrossRef]
21. Kan, X.; Wei, L.; Li, X.; Li, H.; Zhou, D.; Yang, W.; Wang, C.-H. Effects of the three dual-fuel strategies on performance and emissions of a biodiesel engine. *Appl. Energy* **2020**, *262*, 114542. [CrossRef]
22. Hirner, F.S.; Hwang, J.; Bae, C.; Patel, C.; Gupta, T.; Agarwal, A.K. Performance and emission evaluation of a small-bore biodiesel compression-ignition engine. *Energy* **2019**, *183*, 971–982. [CrossRef]
23. Li, H.; Yang, W.; Zhou, D.; Yu, W. Numerical study of the effects of biodiesel unsaturation on combustion and emission characteristics in diesel engine. *Appl. Therm. Eng.* **2018**, *137*, 310–318. [CrossRef]
24. Ramalingam, S.; Rajendran, S.; Ganesan, P.; Govindasamy, M. Effect of operating parameters and antioxidant additives with biodiesels to improve the performance and reducing the emissions in a compression ignition engine—A review. *Renew. Sustain. Energy Rev.* **2018**, *81*, 775–788. [CrossRef]
25. Ewunie, G.A.; Morken, J.; Lekang, O.I.; Yigezu, Z.D. Factors affecting the potential of *Jatropha curcas* for sustainable biodiesel production: A critical review. *Renew. Sustain. Energy Rev.* **2020**, *137*, 110500. [CrossRef]
26. Liu, Z.-W.; Li, F.-S.; Wang, W.-C.; Wang, B.-C. Impact of different levels of biodiesel oxidation on its emission characteristics. *J. Energy Inst.* **2018**, *92*, 861–870. [CrossRef]
27. Fattah, I.R.; Masjuki, H.; Kalam, M.; Wakil, M.; Rashedul, H.; Abedin, M. Performance and emission characteristics of a CI engine fueled with *Cocos nucifera* and *Jatropha curcas* B20 blends accompanying antioxidants. *Ind. Crops Prod.* **2014**, *57*, 132–140. [CrossRef]
28. Ryu, K. The characteristics of performance and exhaust emissions of a diesel engine using a biodiesel with antioxidants. *Bioresour. Technol.* **2010**, *101*, S78–S82. [CrossRef]
29. Jain, S.; Sharma, M. Engine performance and emission analysis using oxidatively stabilized *Jatropha curcas* biodiesel. *Fuel* **2013**, *106*, 152–156. [CrossRef]
30. Agarwal, A.K.; Shrivastava, A.; Prasad, R.K. Evaluation of toxic potential of particulates emitted from Jatropha biodiesel fuelled engine. *Renew. Energy* **2016**, *99*, 564–572. [CrossRef]
31. Rao, M.S.; Anand, R. Performance and emission characteristics improvement studies on a biodiesel fuelled DICI engine using water and AlO(OH) nanoparticles. *Appl. Therm. Eng.* **2016**, *98*, 636–645. [CrossRef]
32. Soudagar, M.E.M.; Nik-Ghazali, N.-N.; Kalam, A.; Badruddin, I.; Banapurmath, N.; Akram, N. The effect of nano-additives in diesel-biodiesel fuel blends: A comprehensive review on stability, engine performance and emission characteristics. *Energy Convers. Manag.* **2018**, *178*, 146–177. [CrossRef]
33. Sui, M.; Chen, Y.; Li, F.; Wang, W.; Shen, J. Study on the mechanism of auto-oxidation of Jatropha biodiesel and the oxidative cleavage of C–C bond. *Fuel* **2021**, *291*, 120052. [CrossRef]

34. Krishania, N.; Rajak, U.; Verma, T.N.; Birru, A.K.; Pugazhendhi, A. Effect of microalgae, tyre pyrolysis oil and Jatropha biodiesel enriched with diesel fuel on performance and emission characteristics of CI engine. *Fuel* **2020**, *278*, 118252. [CrossRef]
35. Nabi, M.; Rasul, M. Influence of second generation biodiesel on engine performance, emissions, energy and exergy parameters. *Energy Convers. Manag.* **2018**, *169*, 326–333. [CrossRef]
36. Lapuerta, M.; Armas, O.; Fernández, J.R. Effect of biodiesel fuels on diesel engine emissions. *Prog. Energy Combust. Sci.* **2008**, *34*, 198–223. [CrossRef]
37. Sharma, A.; Singh, Y.; Singh, N.K.; Singla, A.; Ong, H.C.; Chen, W.-H. Effective utilization of tobacco (Nicotiana Tabaccum) for biodiesel production and its application on diesel engine using response surface methodology approach. *Fuel* **2020**, *273*, 117793. [CrossRef]
38. Aydın, S. Comprehensive analysis of combustion, performance and emissions of power generator diesel engine fueled with different source of biodiesel blends. *Energy* **2020**, *205*, 118074. [CrossRef]
39. Oni, B.A.; Oluwatosin, D. Emission characteristics and performance of neem seed (*Azadirachta indica*) and Camelina (*Camelina sativa*) based biodiesel in diesel engine. *Renew. Energy* **2020**, *149*, 725–734. [CrossRef]
40. Mishra, S.; Chauhan, A.; Mishra, K.B. Role of binary and ternary blends of WCO biodiesel on emission reduction in diesel engine. *Fuel* **2019**, *262*, 116604. [CrossRef]
41. Subramaniam, M.; Solomon, J.M.; Nadanakumar, V.; Anaimuthu, S.; Sathyamurthy, R. Experimental investigation on performance, combustion and emission characteristics of DI diesel engine using algae as a biodiesel. *Energy Rep.* **2020**, *6*, 1382–1392. [CrossRef]
42. Mirhashemi, F.S.; Sadrnia, H. NOX emissions of compression ignition engines fueled with various biodiesel blends: A review. *J. Energy Inst.* **2019**, *93*, 129–151. [CrossRef]